

Double-plasmon excitations in the alkali metals

This article has been downloaded from IOPscience. Please scroll down to see the full text article.

2009 J. Phys. A: Math. Theor. 42 214036

(<http://iopscience.iop.org/1751-8121/42/21/214036>)

View [the table of contents for this issue](#), or go to the [journal homepage](#) for more

Download details:

IP Address: 171.66.16.154

The article was downloaded on 03/06/2010 at 07:49

Please note that [terms and conditions apply](#).

Double-plasmon excitations in the alkali metals

H M Böhm, R Holler, E Krotscheck and M Panholzer

Institute of Theoretical Physics, Johannes Kepler University, Altenbergerstr 69, A-4040 Linz, Austria

E-mail: helga.boehm@jku.at

Received 15 October 2008, in final form 11 March 2009

Published 8 May 2009

Online at stacks.iop.org/JPhysA/42/214036

Abstract

We calculate the excitation spectrum of the electron liquid using the formalism of correlated basis functions including time-dependent pair correlations. Using the static structure factor of the ground state as sole input, our formalism is naturally suited for studying correlation effects on the energy loss function. The most prominent example is the double plasmon, for which our results are in good agreement with recent experiments on various alkali metals.

PACS numbers: 71.10.Ca, 71.10.Li, 71.45.Gm

1. Introduction

Recent inelastic x-ray scattering measurements [1, 2] have renewed the interest in the dynamic excitation spectrum of the electron liquid, a successful reference model for various charged systems [3]. A shoulder was detected on the high energy side of the dynamic structure factor $S(q, \omega)$. Computations of the leading proper polarization Feynman diagrams outside the particle-hole continuum performed by Sturm and Gusarov [4] show that this structure in $S(q, \omega)$ can be attributed to a correlation-induced double-plasmon excitation.

For the ground state, a most powerful approach starts with a Jastrow ansatz for the wavefunction, including correlations in a physically intuitive way from the start,

$$|\Psi_0\rangle \equiv F|\Phi_0\rangle = \exp\left\{\frac{1}{2}\left(\sum_i u^{(1)}(\mathbf{r}_i) + \sum_{i<j} u^{(2)}(\mathbf{r}_i, \mathbf{r}_j) + \dots\right)\right\}|\Phi_0\rangle. \quad (1)$$

Here, Φ_0 denotes a Slater determinant and $u^{(n)}$ are determined by *functionally* minimizing the energy $E_0 = \langle\Psi_0|H|\Psi_0\rangle$. At the level of $u^{(3)}$, for charged bosons [5] this yields a numerically small energy correction, equivalent to the sum of individually rather large contributions of many Feynman diagrams. We are thus confident that optimizing the action for the generalization of (1) to excited states,

$$|\Psi_t\rangle = \frac{e^{-iE_0t/\hbar}}{\sqrt{\mathcal{N}}} F e^{\delta U(t)} |\Phi_0\rangle, \quad \mathcal{N} \equiv \langle\Psi_t|\Psi_t\rangle \quad (2a)$$

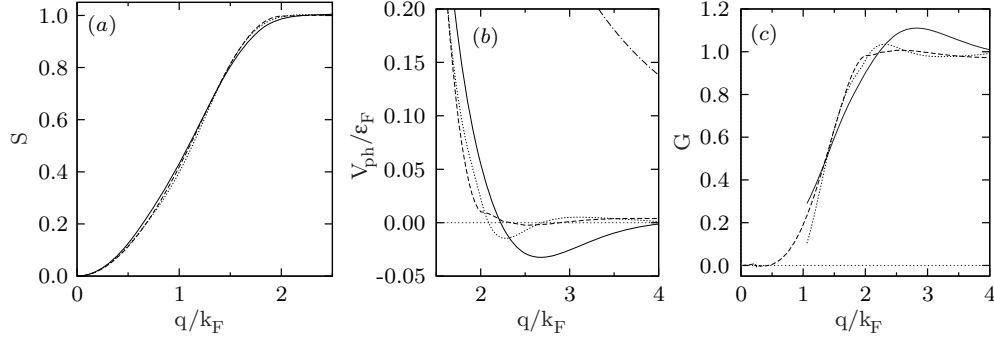


Figure 1. (a) Static structure factor, (b) particle–hole interaction and (c) local field correction from $V_{\text{ph}} \equiv (1 - \mathcal{G}(q))v^{\text{C}}$. The curves result from using the data from MC (full lines [6], short dashed lines [9]) and from FHNC (dashed lines [7]); the dash-dotted line in (b) is the Coulomb potential. The density $\rho = 3/(4\pi a_{\text{B}}^3 r_s^3)$ corresponds to $r_s = 5$.

$$\delta U(t) = \sum_{ph} \delta u_{ph}^{(1)}(t) a_p^\dagger a_h + \frac{1}{2} \sum_{pp'hh'} \delta u_{pp'hh'}^{(2)}(t) a_p^\dagger a_{p'}^\dagger a_{h'} a_h + \dots, \quad (2b)$$

again properly captures the relevant physics in an optimal way.

Aiming at explaining the excitation spectrum, we use the ground-state static structure factor $S(q)$ as sole input for our theory, taken either from recent Monte Carlo (MC) [6] or from hypernetted chain (FHNC) [7] computations. Neglecting dynamic pair correlations $\delta u^{(2)}(t)$ in (2b) reproduces the random phase approximation (RPA) with the Coulomb interaction v^{C} replaced by V_{ph} ($S_{\text{F}}(q)$ is the free static structure factor)

$$V_{\text{ph}}(q) = \frac{\hbar^2 q^2}{4m} \left[\frac{1}{S^2(q)} - \frac{1}{S_{\text{F}}^2(q)} \right]. \quad (3)$$

Figure 1 shows that these interactions are noticeably different despite the close agreement of the MC and FHNC data for $S(q)$. The corresponding static local field correction $\mathcal{G}(q)$ does not show the correct large q behavior [3, 8], reflecting the necessity to include higher order dynamic correlations even for obtaining the correct $\omega = 0$ response.

2. Formalism

The equations of motion for the correlation amplitudes $\delta u^{(n)}(t)$ yield a linear density–density response function that takes the following form [10, 11]:

$$\chi(q, \omega) = \chi^s(q, \omega) / [1 - V_{\text{ph}}(q)\chi^s(q, \omega) - \Lambda(q, \omega)]. \quad (4)$$

Though a clear-cut distinction between single-particle (sp) and pair properties is ambiguous in quantum systems, important arguments have been given [12, 13] that certain sp properties are most suitably accounted for in the numerator of χ (in contrast to including them in a ‘local field correction’ $\mathcal{G}(q, \omega)$). Our formalism gives an additive correction to the Lindhard function $\chi^0 = \chi^{0+} + \chi^{0-}$ in the numerator,

$$\chi^s(q, \omega) = \chi^0 - \chi^{0+} \chi^{0-} (\mathcal{A}^+ + \mathcal{A}^-), \quad \chi^{0\pm} \equiv \frac{1}{N} \sum_{\mathbf{h}} \frac{n_{\mathbf{h}} (1 - n_{\mathbf{h}+\mathbf{q}})}{\pm \hbar \omega - (e_{\mathbf{h}+\mathbf{q}} - e_{\mathbf{h}})} \quad (5)$$

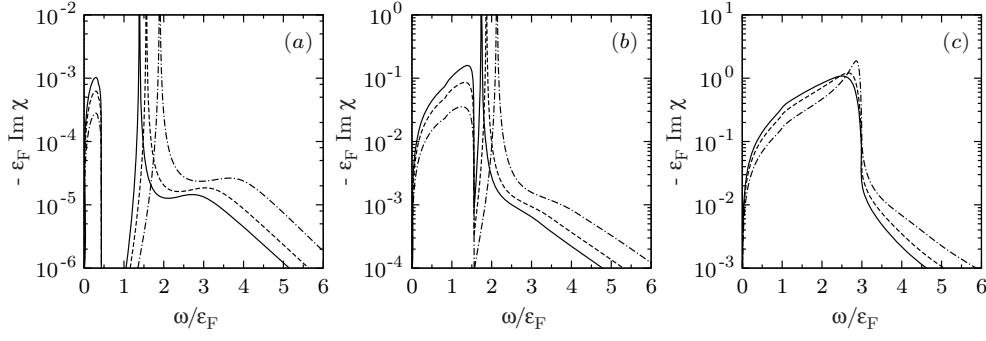


Figure 2. Dynamic structure factor for three typical wave vectors (measured in Fermi wave vectors k_F), (a) $q = 0.2$, (b) $q = 0.4$ and (c) $q = 1.0$, based on the FHNC [7] input. The densities correspond to the experimentally investigated simple metals, Al ($r_s = 2.06$, full line), Mg ($r_s = 2.66$, short-dashed line) and Na ($r_s = 3.99$, chained line).

(where N is the particle number, $e_{\mathbf{k}} = \hbar^2 k^2 / 2m$; $n_{\mathbf{k}}$ are the free Fermi functions). Using the pair analogues $\mu^{0\pm}$ [11] of the partial Lindhard functions $\chi^{0\pm}$, the direct correlation function $X(q) = 1/S_F(q) - 1/S(q)$, and the definition $-\mathbf{q}'' = \mathbf{q} + \mathbf{q}'$, we obtain

$$\Lambda = \frac{S^2 + S_F^2}{4SS_F} \chi^0(\mathcal{A}^+ + \mathcal{A}^-) + \frac{1}{2}(\chi^{0+} - \chi^{0-})(\mathcal{A}^+ - \mathcal{A}^-) - \chi^{0+} \chi^{0-} \mathcal{A}^+ \mathcal{A}^-, \quad (6)$$

$$\mathcal{A}^\pm(q, \omega) = \frac{1}{2N} \sum_{\mathbf{q}'} |W_{q, \mathbf{q}', \mathbf{q}''}|^2 \mu_{q'q''}^{0\pm}(\hbar\omega \pm e_{q'} X(q') \pm e_{q''} X(q'')), \quad (7)$$

and a lengthy expression¹ for the vertex $W_{q, \mathbf{q}', \mathbf{q}''}$.

A common simplification is to approximate the fermionic χ^0 by a single-mode function; this in turn leads to χ^{RPA} being replaced by the plasmon–pole approximation χ^{PPA} with excitations at the Bijl–Feynman energies $\varepsilon_q \equiv e_q/S(q)$. The analogous procedure for the pair Lindhard function μ^0 gives

$$\mu_{q'q''}^{0\pm}(\omega \pm e_{q'} X(q') \pm e_{q''} X(q'')) \rightarrow \frac{S_F(q') S_F(q'')}{\pm \hbar\omega - \varepsilon_{q'} - \varepsilon_{q''}}, \quad (8)$$

with obviously a pole at a ‘double-Feynman excitation’ (a double plasmon for $q \rightarrow 0$).

3. Results

In figure 2 we show $\text{Im } \chi = \frac{-\pi}{\hbar N} S(q, \omega)$ for q values where the plasmon is (a) well outside the sp continuum, (b) close to entering it, and, finally, (c) fully Landau damped. The finite width in (a) and (b) is due to decay into pair excitations. Our results are very close for both the MC and FHNC input data, despite the differences seen in V_{ph} in figure 1(b).

To the right of the main (i.e. plasmon-) peak in figures 2(a) and (b) a shoulder arises from a double-plasmon excitation; in (c) it is visible only for the largest r_s -value. Obviously, with increasing q determining the exact position of this peak becomes difficult. In [2] this was achieved by subtracting an experimentally fitted tail from the spectra. We here prefer

¹ See [11], appendix B. The fermionic $W_{q, \mathbf{q}', \mathbf{q}''}$ reduces to the much simpler equation (17) of [11] in the bosonic limit, which was first derived in [14].

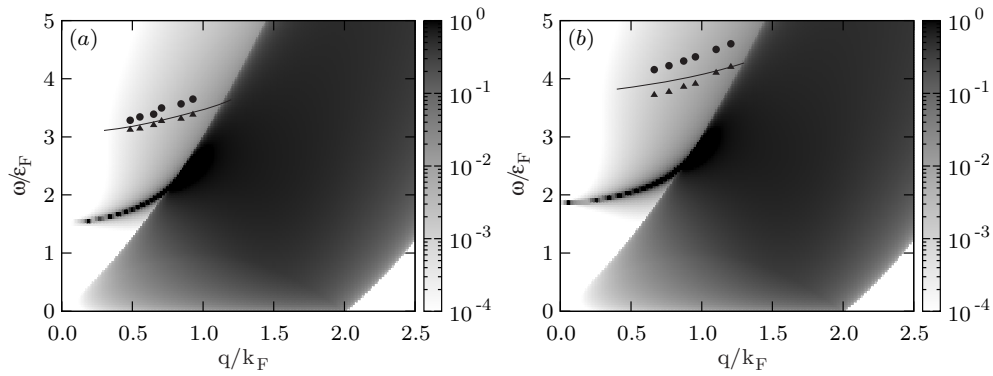


Figure 3. Dynamic structure factor (log scale) for (a) Mg ($r_s = 2.66$) and (b) Na ($r_s = 3.99$, room temperature experiments). Full line: our theoretical double-plasmon peak; triangles: experiment [2]; circles: theory of [2, 4] (from Feynman diagrams).

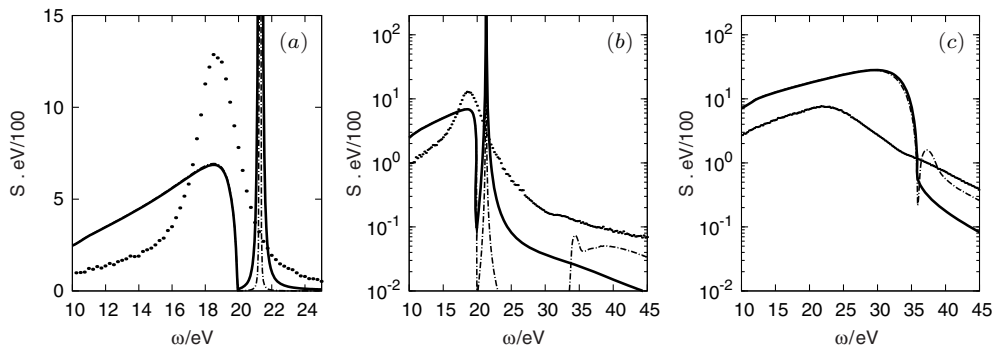


Figure 4. IXS data of Al (points) and present theory (full line), the broken line is obtained with equation (8). In (a) the experimental data were scaled by a factor 0.4; (b) and (c) show $\log S(q, \omega)$. The wave vector q/k_F is 0.64 in (a) and (b) and 1.01 in (c).

to take advantage of expression (8). Figure 3 shows the comparison of the resulting double-plasmon peak with the experimental one. We attribute the slightly different dispersion to the ambiguity of exactly determining the peak position. The remarkably good agreement with the measurements shows that our approach indeed models the essential physics of dynamic correlations.

Finally, in figure 4 we compare the calculated and measured $S(q, \omega)$ for Al (we rescale the experimental data to give the same well-known $S(q)$ [6, 7]). At $q = 0.64k_F$ we find the plasmon essentially at its RPA position, substantially broadened due to decay into pair excitations, but well separated from the single-particle-hole continuum. By contrast, the main experimental peak is found 13% below the RPA value with no distinction from particle-hole excitations. However, the spectrum in this region is largely influenced by band-structure effects [15]. The situation is similar in Na.

References

- [1] Sternemann C, Huotari S, Vankó G, Volmer M, Monaco G, Gusarov A, Sturm H L K and Schülke W 2005 *Phys. Rev. Lett.* **95** 157401

- [2] Huotari S, Sternemann C, Schülke W, Sturm K, Lustfeld H, Sternemann H, Volmer M, Gusarov A, Müller H and Monaco G 2008 *Phys. Rev. B* **77** 195125
- [3] Giuliani G and Vignale G 2005 *Quantum Theory of the Electron Liquid* (Cambridge: Cambridge University Press)
- [4] Sturm K and Gusarov A 2000 *Phys. Rev. B* **62** 16474–91
- [5] Apaja V, Halinen J, Halonen V, Krotscheck E and Saarela M 1997 *Phys. Rev. B* **55** 12925–45
- [6] Gori-Giorgi P, Sacchetti F and Bachelet G B 2000 *Phys. Rev. B* **61** 7353–63
- [7] Krotscheck E 1984 *Ann. Phys. (NY)* **155** 1–55
- [8] Moroni S, Ceperley D M and Senatore G 1995 *Phys. Rev. Lett.* **75** 689–92
- [9] Ortiz G and Ballone P 1994 *Phys. Rev. B* **50** 1391–405
- [10] Böhm H M, Krotscheck E and Panholzer M 2007 *J. Low Temp. Phys.* **148** 139–43
- [11] Böhm H M, Holler R, Krotscheck E and Panholzer M 2008 *Int. J. Mod. Phys. B* **22** 4655–65
- [12] March N H and Tosi M P 1984 *Coulomb Liquids* (London: Academic) pp 463–82
- [13] Neilson D, Swierkowski L, Sjölander A and Szymanski J 1991 *Phys. Rev. B* **44** 6291–305
- [14] Chang C C and Campbell C E 1976 *Phys. Rev. B* **13** 3779–82
- [15] Huotari S 2008 private communication